

1 **SUPPLEMENTAL DATA FILE**

2
3 **Title:** *Survival Advantage of MCL Cells with PIK3CA gain or PTEN Loss Is Mediated By Decreased*
4 *Dependence on B-Cell Receptor Signaling and Increased Survival after BCL2 Inhibition and Under*
5 *Hypoxia*

6
7 **Authors:** Nardjas Bettazova^{1,2}, Jana Senavova,^{3,4} Kristyna Kupcova^{3,4}, Dana Sovilj^{5,6}, Anezka
8 Rajmonova⁴, Ladislav Andera^{5,6}, Karla Svobodova⁷, Adéla Berkova⁷, Zuzana Zemanova⁷, Lenka
9 Daumova¹, Vaclav Herman^{3,4}, Alexandra Dolnikova¹, R. Eric Davis⁸, Marek Trneny³, Pavel Klener*^{1,3}, and
10 Ondrej Havranek^{3,4}

11
12 ¹Institute of Pathological Physiology, First Faculty of Medicine, Charles University, Prague, Czech
13 Republic

14 ²Department of Medical Genetics, Third Faculty of Medicine, Charles University, Prague, Czech
15 Republic

16 ³First Department of Medicine-Department of Hematology, Charles University General Hospital in
17 Prague, Czech Republic

18 ⁴BIOCEV LF1- Biotechnology and Biomedicine Centre, First Faculty of Medicine, Charles University,
19 Prague, Czech Republic

20 ⁵Institute of Biotechnology BIOCEV, Czech Academy of Sciences, Prague, Czech Republic

21 ⁶Institute of Molecular Genetics, Czech Academy of Sciences, Prague, Czech Republic

22 ⁷Center for Oncocytogenetics, Institute of Medical Biochemistry and Laboratory Diagnostics, Charles
23 University and General University Hospital, Prague, Czech Republic

24 ⁸Department of Lymphoma and Myeloma, The UT MD Anderson Cancer Center, Houston, TX, U.S.A

25
26 ***Corresponding author:**

27 Pavel Klener, Institute of Pathological Physiology, First Faculty of Medicine, Charles University, Prague,
28 Czech Republic

29 email: pavel.klener2@lf1.cuni.cz

30 **SUPPLEMENTAL MATERIALS AND METHODS**

31

32 *Cell lines and patient samples*

33 MINO, Z138, UPF1H, UPF19U, JEKO-1 cell lines with transgenic *PIK3CA* (over)expression (*PIK3CA* UP)
34 or with *PTEN* knock-out (*PTEN* KO) were derived as described below. Cells were maintained in Iscove's
35 modified Dulbecco's medium (IMDM) supplemented with 15% fetal bovine serum (FBS) and 1%
36 penicillin/streptomycin. Primary MCL cells were obtained from leukemized blood, infiltrated lymph
37 nodes, malignant ascites, pleural effusion, and infiltrated bone marrow of 28 patients with so far
38 untreated or relapsed / refractory (R/R) MCL. Approval was obtained from all patients according to the
39 (WMA) Declaration of Helsinki. The project was approved by the institutional ethics committee of the
40 General University Hospital in Prague under number 60/20.

41

42 *Cytotoxic agents*

43 Specific PI3K inhibitors including idelalisib (PI3K δ inhibitor), duvelisib (PI3K/ γ δ inhibitor), AZD8835
44 (PI3K α/δ inhibitor), AZD8186 (PI3K β/δ inhibitor), alpelisib (PI3K α inhibitor), copanlisib (pan-PI3K
45 inhibitor), and others; capivasertib (pan-AKT inhibitor), ibrutinib (BTK inhibitor), venetoclax (BCL2
46 inhibitor), S63854 (MCL1 inhibitor), and A1155463 (BCL-XL inhibitor) were purchased from
47 MedChemExpress. 2-Deoxy-D-Glucose (2-DG, inhibitor of glycolysis) was provided by SIGMA.

48

49 *Cytogenomic analyses*

50 I-FISH analyses were performed with commercially available DNA probes SPEC PIK3CA/CEN 3 DC
51 (**ZytoVision GmbH, Bremerhaven, Germany**), Vysis LSI PTEN/CEP 10 and Vysis LSI TP53 (17p13.1)/CEP
52 17 (Abbott Molecular, Des Plaines, IL, USA) according to the manufacturers' protocols. At least 200
53 interphase nuclei were analyzed by two independent observers. The cut off level for positive values
54 were determined on samples obtained from 10 cytogenetically normal persons and were found to be
55 5% (mean \pm 3SD) for losses (deletions, monosomies), and 2.5% (mean \pm 3SD) for gains (trisomies,
56 amplifications). aCGH/SNP analyses were performed with a SurePrint G3 Cancer CGH+SNP Microarray,
57 4x180K (Agilent Technologies, Santa Clara, USA) . The QIAamp DNA Blood Mini Kit (Qiagen Inc., Hilden,
58 Germany) was used to isolate genomic DNA from bone-marrow cells stored in fixative. The
59 concentration and quality of the isolated DNA were confirmed with a NanoDrop 2000
60 spectrophotometer (Thermo Fisher Scientific, Waltham, MA). The array slides were scanned with a
61 microarray scanner system (G2565CA, Agilent Technologies) and analyzed with Agilent Cytogenomics
62 v5.2.0.20 software (Agilent Technologies).

63

64 *Generation of cell lines with target genes knock out/knock down*

65 *PTEN* KO was generated using CRISPR/Cas9 system exactly as we did before(1). Briefly, we combined
66 double strand DNA cut at the *PTEN* translation initiation site and provided repair template plasmid for
67 homologous repair (HR) based insertion of GFP-STOP-pA DNA sequence. In result, GFP is expressed
68 instead of *PTEN* and serves as a marker for viable sorting of *PTEN* KO cells. To introduce double strand
69 DNA break at the *PTEN* translation initiation site, we used a “paired nickases” approach(2). *PTEN* target
70 sequences (*PTEN*_1 TTGACCTGTATCCATTTCTGCGG and *PTEN*_2 TTGATGATGGCTGTCATGTCTGG) were
71 cloned into a chimeric plasmids pX335-U6-Chimeric_BB-CBh-hSpCas9n(D10A), coding for Cas9 D10A
72 as well as gRNA (Addgene plasmid #42335)(3) and co-electroporated (see below) them with the above-
73 mentioned HR repair template plasmid(1). Western blotting of bulk sorted GFP positive / *PTEN* KO cells
74 confirmed *PTEN* KO in UPF1H, Z138, and JEKO-1 cells (Figure 1A and Supplemental Figure 1) and
75 showed *PTEN* KD in MINO and UPF19U (resulting from heterozygotic KO, Supplemental Figure 1). To
76 generate MINO *PTEN* KO cells, bulk sorted GFP positive cells were single cell cloned to obtain pure
77 *PTEN* KO cells (confirmed by western blotting, Figure 1A). If necessary for consequent AKT activity
78 measurement (see below), GFP was knocked out using similar CRISP/Cas9 system with single GFP
79 target sequence (GGGCGAGGAGCTGTTCACCGGGG) cloned into a pX330-U6-Chimeric_BB-CBh-
80 hSpCas9 (Addgene plasmid # 42230, coding for Cas9 as well as gRNA)(3). GFP negative *PTEN* KO cells
81 were then sorted to purity for consequent analyses(4). BCR KO cells were generated as we did
82 previously(1). We used gRNAs targeting the constant region of immunoglobulin heavy (IgH) chain of
83 cell line specific BCR isotype. We used the above mentioned px330 plasmid with the following IgH M
84 target sequence for all tested cell lines: AGATGAGCTTGGACTTGCAGGGG. The BCR KO cell growth and
85 the change of their proportion in cell culture was measured starting three days after electroporation
86 using flow cytometry (staining the BCR with anti-human IgM FITC antibody, ThermoFisher Scientific
87 #H15001). Comparison of growth rates of genetically modified cells was performed using a bead assay
88 as described previously(1).

89

90 *Generation of cell lines with target genes overexpression*

91 Similarly as we did before, we have used the sleeping beauty transposon system(5) for stable
92 overexpression of *PIK3CA* and to express the AKT activity reporter (see below) in selected cell lines(1,
93 6). Briefly, the WT *PIK3CA* cDNA was cloned into donor plasmid pSBbi Pur (Addgene plasmid #60523)(5)
94 and AKT activity reporter was cloned into pSBbi-Pur (Addgene plasmid #60523)(5) or pSBbi-Neo
95 (Addgene plasmid #60525)(5) donor plasmids. These donor plasmids (6 µg) were co-electroporated
96 with 4 µg of transposase coding plasmid pCMV(CAT)T7-SB100 (Addgene plasmid #34879)(7). After
97 three days of culture without antibiotics, selection with appropriate antibiotics was initiated with the

98 following concentrations: puromycin at final concentration of 2 $\mu\text{g}/\text{mL}$ and geneticin at final
99 concentration of 200 $\mu\text{g}/\text{mL}$.

100

101 *Measurement of AKT activity in living cells*

102 To measure AKT activity in live cells, we used a genetically encoded Förster resonance energy transfer
103 (FRET) biosensor as we developed and used before(1, 4). The AKT activity reporter (Lyn-Akt AR2-EV,
104 Addgene plasmid #125199) has the following structure: cell membrane targeting sequence (from Lyn)
105 - mCerulean3 - FHA1 phospho-amino acid binding domain – EV flexible linker – part of FOXO domain
106 (naturally phosphorylated by AKT) - cpVenus[E172]. AKT mediated phosphorylation of its FOXO part
107 leads to its binding to FHA1 domain, change in reporter confirmation, and increase in FRET. As we
108 published previously, we have used flow cytometry for FRET measurement in living cells using in house
109 R package (fRet) to calculate the absolute FRET efficiency (E) values reflecting the AKT activity(1, 4).
110 FRET measurement and calculations were performed as per the fRet package manual using cells
111 expressing appropriate calibration controls: mCerulean3 only, cpVenus[E172] only, FRET high control,
112 and FRET low control (to calculate necessary set up dependent coefficients for each individually
113 performed experiment)(4).

114 To compare cells with *PTEN* KO or *PIK3CA* UP to their parental counterparts, five hundred thousand
115 cells per sample were resuspended in fresh media, incubated one hour in regular cell culture incubator
116 (37°C with 5% of CO_2), and FRET measured for each sample immediately after removing them from the
117 incubator using flow cytometry (Cytoflex, Beckma Coulter). To measure the AKT activity after ibrutinib
118 treatment, five hundred thousand cells per each sample were pre-incubated (37°C with 5% of CO_2) for
119 3 hours with the ibrutinib concentration of 1 μM and 0.1 μM in total amount of 3ml cell culture cell
120 media directly in flow cytometry tubes and FRET measured for each sample immediately after removal
121 from the incubator using flow cytometry (Cytoflex, Beckma Coulter).

122

123 *Apoptosis and proliferation assays*

124 Apoptosis was measured by standard Annexin-V / propidium iodide (PI) assay. Briefly, on day 1 the
125 cells were resuspended into 96-well plate (100 000 cells per well). Each drug was added in 3 different
126 concentrations. After 24 hours of incubation, Annexin V FITC (Exbio) and PI (Sigma) were added to
127 detect apoptotic and necrotic cells. The measurements were carried out by flow cytometry (BD FACS
128 CANTO II). The percentage of necrotic and apoptotic cells was calculated as previously reported(6).

129 Proliferation was measured by commercially available WST-8 based cell proliferation assay according
130 to the manufacturer's recommendations. Briefly, on day 1, the cells were resuspended into 96-well
131 plate (50 000 – 100 000 cells per well). The tested PI3K and AKT inhibitors were added at
132 concentrations 1 and 10 μM (Copanlisib at 0,01 and 0,1 μM), BTK inhibitor at 0,1 and 1 μM and BCL2

133 family inhibitors at 0,01, 0,1 and 1 μ M. After 72 hours of incubation, WST-8 reagent from Quick Cell
134 Proliferation Assay Kit (BioVision) was added, for a further 3 hours incubation. Absorbance of samples
135 was measured on ELISA reader. The proliferation curve was calculated as previously reported(8).

136

137 *Western blotting*

138 Samples were lysed in RIPA buffer (150 mM NaCl, 0,1 % SDS,1mM EDTA,0,5% Sodium Deoxycholate,
139 1% Triton X-100, pH 7.4). A protease (Sigma) and a phosphatase inhibitor (Roche) were added. Protein
140 concentration was determined using Pierce BCA Protein Assay (ThermoFisher scientific) .20 μ g of
141 sample was mixed with laemelli sample buffer (BioRAD) containing mercaptoethanol and boiled for 5
142 min. Duplicate samples were separated on 10%,12% and 15% SDS-PAGE gels. After electrophoresis,
143 proteins were blotted onto 0.22 μ M PVDF membranes (advansta). Membranes were incubated for 1 h
144 in 1xPBS containing 0.1% Tween-20 and 5% non-fat dried milk. Samples were incubated with primary
145 antibodies overnight then with secondary antibodies for 30 min. To detect bands WesternBright ECL
146 HRP substrate (advansta) was used. The membranes were imaged by ChemiDoc™MP Imaging system
147 (BioRAD). The following antibodies were used in our study: PIK3CA (# 4249), PTEN (# 5384), phospho-
148 PTEN ser 380 (# 9551), total AKT (# 9272), phospho-AKT ser 473 (# 4060), FOXO3A (# 12829), phospho-
149 FOXO3A ser 253 (# 9466), GSK3- β (# 12566), phospho-GSK3- β ser 9 (# 9336), BIM (# 2933), BAK (#
150 12105), BAX (# 2774), BCL-XL (# 2764), MCL1 (# 39224) , phospho-BAD ser 136 (# 9295) and HIF1 α (#
151 14179)were from Cell Signaling technology. B-Actin (# 6276), c-MYC (# 32072), and α -Tubulin (# 7291)
152 from ABCAM. BCL2 (# 610539) from BD Transduction Laboratories.BCL2 (#783) from SantaCruz.
153 GAPDH (# G8795) from SIGMA. BAD polyclonal (# PA5-11403) from Thermo-Fisher Scientific. NOXA
154 polyclonal (# 2437) from ProSci. The densitometric analysis was carried out by Image-Lab Bio-Rad-6.1
155 software and adjusted total volume values were used for quantification.

156

157 *Coimmunoprecipitation assay*

158 The immunoprecipitation was performed according to the previously mentioned protocol (9). Anti-
159 BAD, Anti-BIM, anti-BID (# 2002) (cell signaling), anti-BAK and anti BAX were used to target the
160 immunoprecipitated anti-Bcl-2 antibody (# 4223) (cell signaling). Anti-BAD, Anti-BIM, anti-BID (# 2002)
161 (cell signaling), anti-BAK and anti BAX were used to target immunoprecipitated anti-BCL-XL antibody
162 (# 32370) (ABCAM)

163

164 *In vitro assays under hypoxia*

165 On day 1, 45×10^4 cells from each cell line resuspended in 3 ml medium were pipetted into two
166 separate 6-well plates. One plate was incubated under normoxic conditions (O_2 concentration=20%)
167 and one plate under hypoxic conditions (O_2 concentration=1%). After 72 h incubation samples were

168 taken from both plates and an apoptosis assay was carried out (for more go to paragraph apoptosis
169 assay)

170

171 *Oxygen Consumption Rate (OCR) and Extracellular Acidification Rate (ECAR) assays*

172 The mito stress test was performed by series of injections, starting with oligomycin (1 μ M, ATP
173 synthase inhibitor), followed by CCCP (2 μ M, mitochondrial uncoupler), and a combination of
174 antimycin and rotenone (0.5 μ M, inhibitors of RCIII and RCI). The glycolytic stress test was run by series
175 of injections, starting with glucose (10mM, substrate of glycolysis), followed by oligomycin (1 μ M,
176 inhibits ATP synthase), and 2-deoxy-D-glucose (50 mM, glycolysis inhibitor). OCR/ECAR were measured
177 after each injection. After the assay, the cells were stained with Hoechst and counted using Cytation5
178 instrument. OCR/ECAR values were normalized to the same cell number.

179 **SUPPLEMENTAL RESULTS**

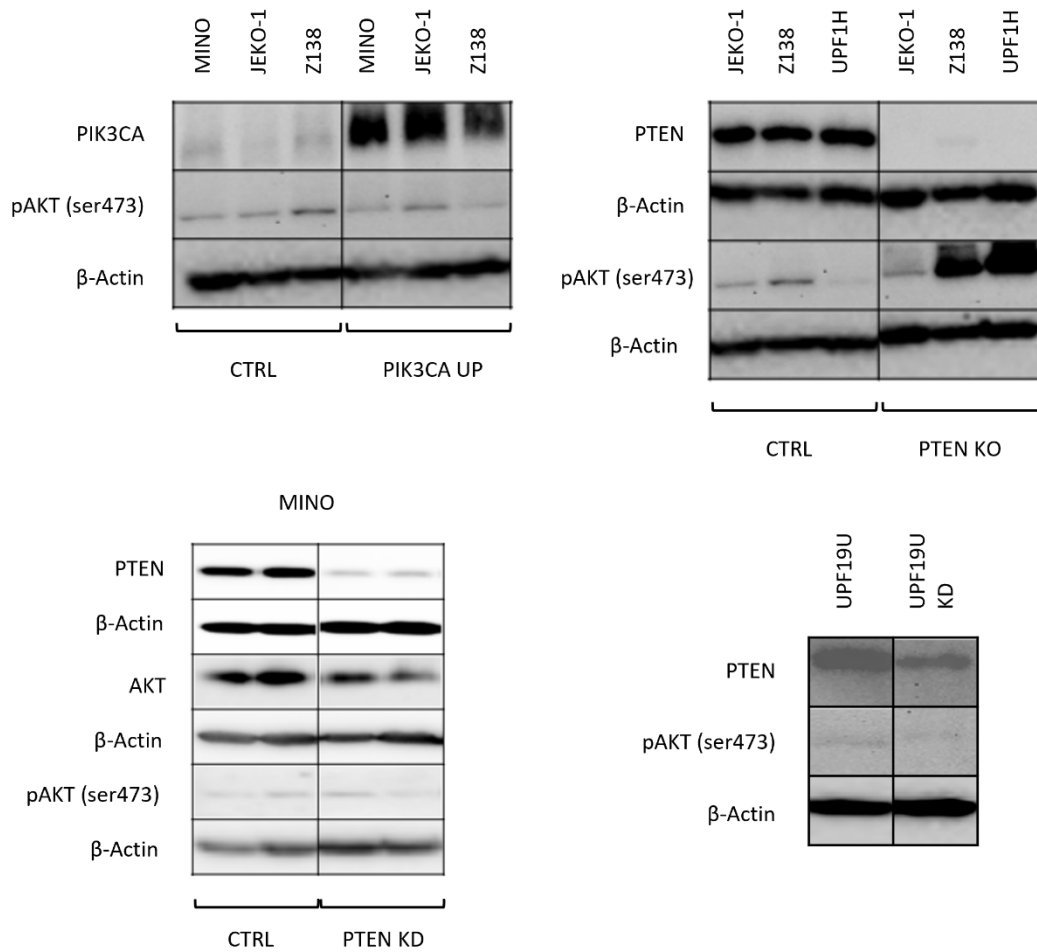
180

181 **Supplemental table 1.** FISH/aCGH of 61 primary MCL patients with > 20% bone marrow infiltration,
 182 43% have *PIK3CA* gain and 7% have *PTEN* monoallelic loss. N/A stands for “not analyzed”.

Patient	FISH or aCGH	<i>PIK3CA</i>	<i>PTEN</i>	<i>TP53</i>
1	aCGH	Gain	N	DEL
2	aCGH	N	N	DEL
3	aCGH	N	DEL	DEL
4	aCGH	N	N	DEL
5	aCGH	Gain	N	N
6	aCGH	N	N	DEL
7	aCGH	N	N	N
8	aCGH	N	N	DEL
9	aCGH	N	N	N
10	aCGH	Gain	N	DEL
11	aCGH	Gain	N	DEL
12	aCGH	N	N	DEL
13	aCGH	N	N	DEL
14	aCGH	N	N	N
15	aCGH	Gain	N	DEL
16	aCGH	Gain	DEL	N/A
17	aCGH	N	N	N
18	aCGH	N	N	DEL
19	aCGH	Gain	N	DEL
20	aCGH	N	N	N
21	aCGH	Gain	N	N
22	aCGH	Gain	N	DEL
23	aCGH	Gain	N	N
24	aCGH	Gain	N	N
25	aCGH	N	N	N
26	aCGH	Gain	N	N
27	aCGH	Gain	N	DEL
28	aCGH	N	N	N
29	aCGH	N	N	N
30	aCGH	Gain	N	N
31	aCGH	Gain	N	N

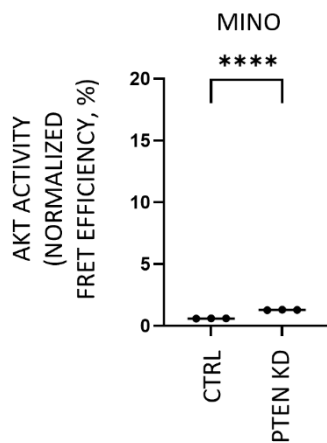
Patient	FISH or aCGH	<i>PIK3CA</i>	<i>PTEN</i>	<i>TP53</i>
32	aCGH	Gain	N	N
33	aCGH	Gain	N	N
34	aCGH	N	N	N
35	aCGH	Gain	N	DEL
36	FISH	Gain	N	N
37	FISH	N	N	DEL
38	FISH	N	N	N
39	FISH	N	N	N
40	FISH	Gain	N	N
41	FISH	N	N	N
42	FISH	N	N	N
43	FISH	Gain	N	N
44	FISH	N	N	N
45	FISH	N	N	N
46	FISH	N	DEL	DEL
47	FISH	Gain	N	N
48	FISH	Gain	N	DEL
49	FISH	N	N	N
50	FISH	Gain	N	N
51	FISH	N	N	N
52	FISH	Gain	N	DEL
53	FISH	Gain	Gain	N
54	FISH	N	N	N
55	FISH	N	N	N
56	FISH	N	DEL	DEL
57	FISH	N	N	DEL
58	FISH	N	N	N
59	FISH	N	N	N
60	FISH	N	N	N
61	FISH	N	N	DEL

183



184

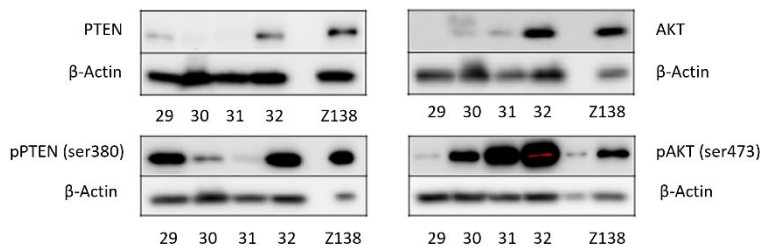
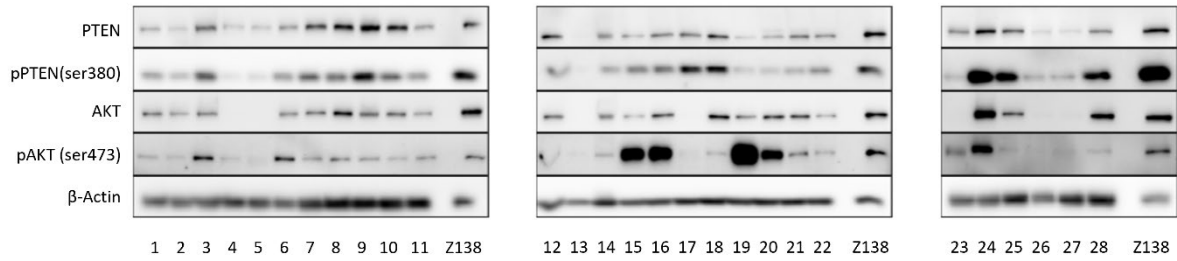
185 **Supplemental figure 1.** Western blots showing overexpression of *PIK3CA* in MINO, JEKO-1, and Z138
 186 *PIK3CA* UP cells, loss of *PTEN* and hyperphosphorylation of AKT in JEKO-1, Z138, and UPF1H *PTEN* KO
 187 cells, and. decreased expression of *PTEN* in MINO and UPF19U *PTEN* KD cells with no changes in the
 188 phosphorylation of AKT. For each sample in MINO versus MINO *PTEN* KD N=2; (N) represents the
 189 number of biological replicates.



190

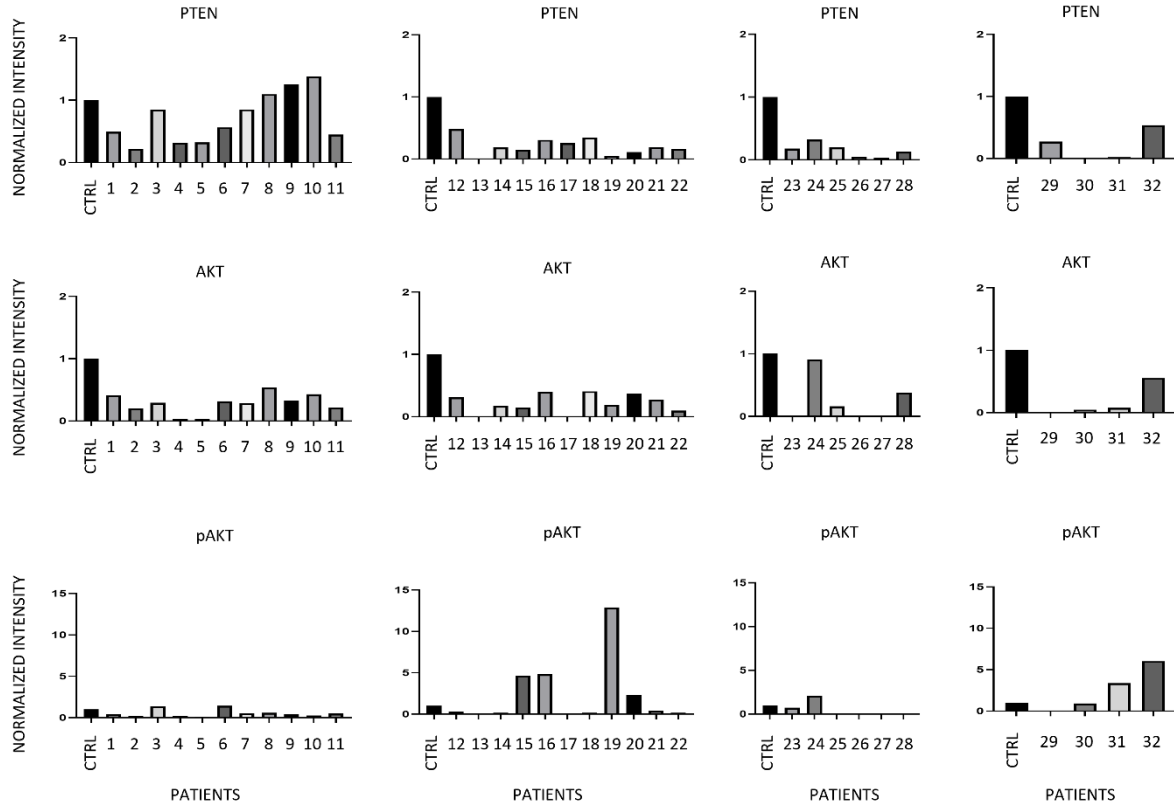
191 **Supplemental figure 2.** AKT activity in MINO *PTEN* KD cells. AKT activity as measured using genetically
 192 encoded FRET-based biosensor. Increased AKT kinase activity in MINO *PTEN* KD cell line is compared
 193 to the respective control cell line, technical triplicates. **** $p < 0.0001$.

194

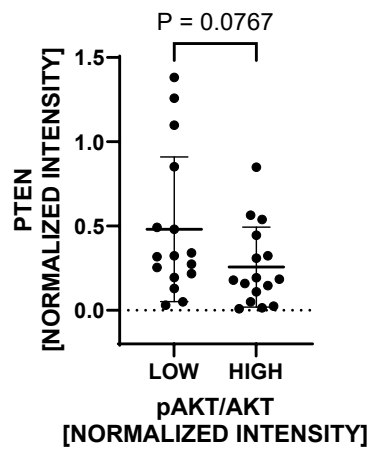


195

196 **Supplemental figure 3.** Western blot analysis of 32 primary MCL samples. Detection of PTEN, pPTEN
 197 (ser380), AKT and pAKT (ser473) expressions. Samples P3, 6, 15, 16, 19, 20, 24, and 32 have lower
 198 expression of *PTEN* and high phosphorylation of AKT. Samples P13, 30, and 31 show complete loss of
 199 *PTEN* with P31 showing hyperphosphorylation of AKT.
 200

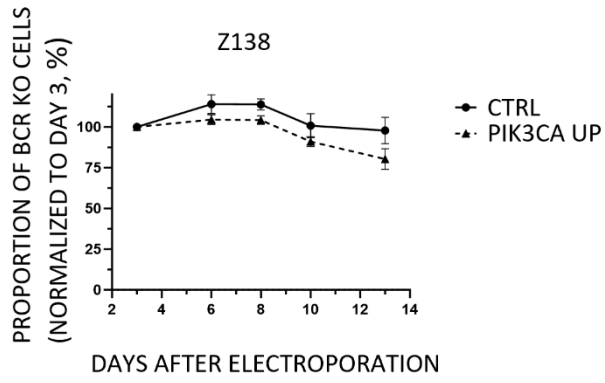


201
202



203

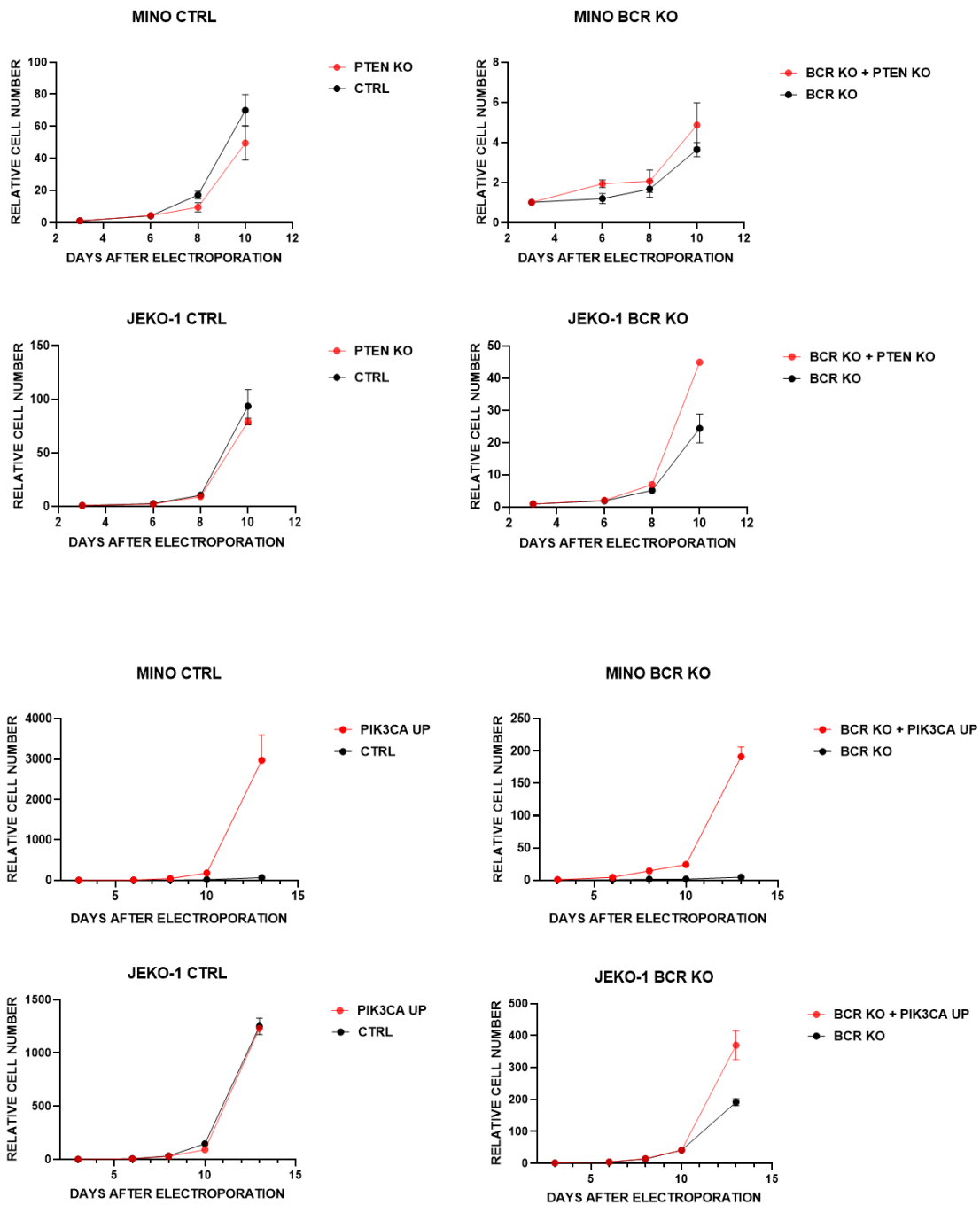
204 **Supplemental figure 4. A.** Quantification of the 32 MCL patients' western blot analysis for PTEN, AKT,
 205 and pAKT (ser473) levels as normalized to the Z138 cell line (CTRL); B. Comparison of PTEN protein
 206 expression levels between pAKT high and low patients' samples based on western blots presented in
 207 Supplemental Figures X and X. Samples were divided into two equal groups based on pAKT levels
 208 (normalized to total AKT) and normalized western blot PTEN intensities were compared. Means and
 209 SD are displayed.



210

211 **Supplemental figure 5.** Knock out of BCR in Z138 cell line demonstrates that Z138 is BCR independent.

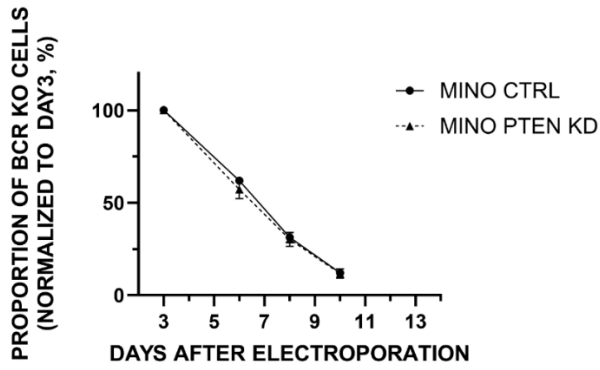
212 Averages of three replicates with SD are displayed.



213

214 **Supplemental figure 6.** PTEN KO slightly decreases the growth of MINO and does not affect the growth
 215 of JEKO-1 CTRL cell lines but slightly increases growth MINO and JEKO-1 BCR KO variants (top panels).
 216 PI3KCA overexpression increases growth of MINO CTRL and as well as MINO BCR KO cells and does not
 217 affect growth of CTRL or BCR KO JEKO-1 cells. Cell growth rates were measured in the same experiment
 218 as presented in Figure 1D and E. ; N=3; data are represented as means \pm SD; (N) represents the number
 219 of biological replicates.

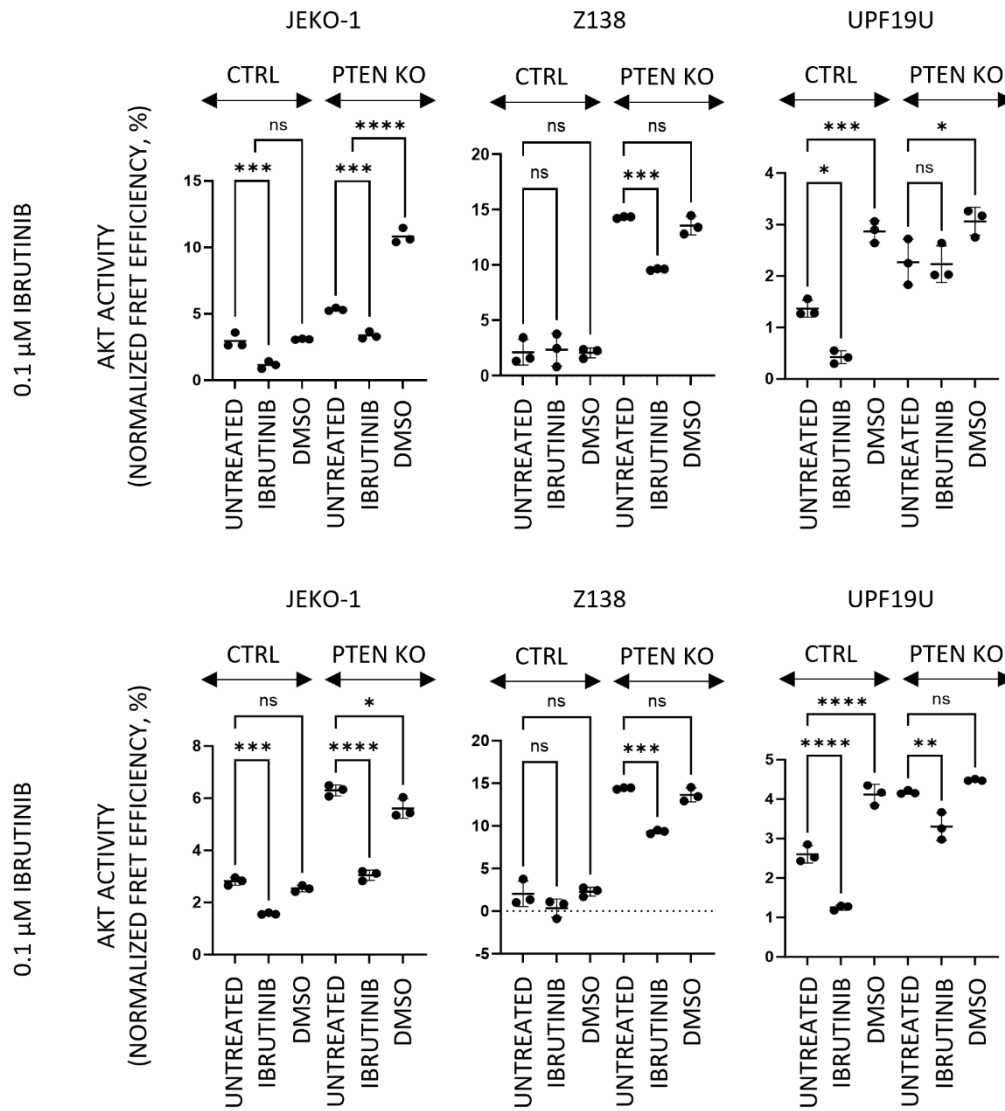
220



221

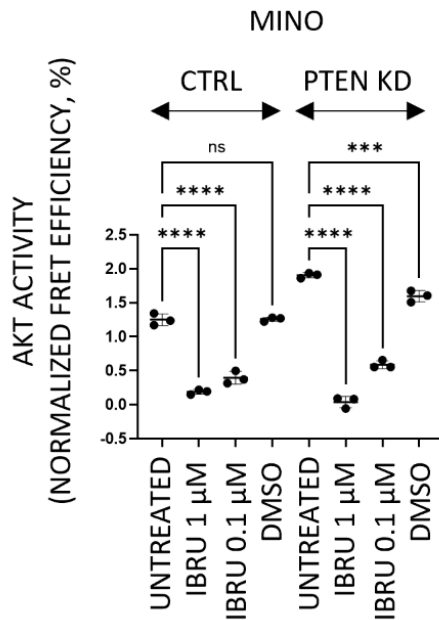
222 **Supplemental figure 7.** PTEN KD does not compensate for the pro-survival signaling from BCR. PTEN
 223 KD did not increase the survival of MCL cells with knockout of BCR gene; N=3; data are represented as
 224 means ± SD; (N) represents the number of biological replicates.

225



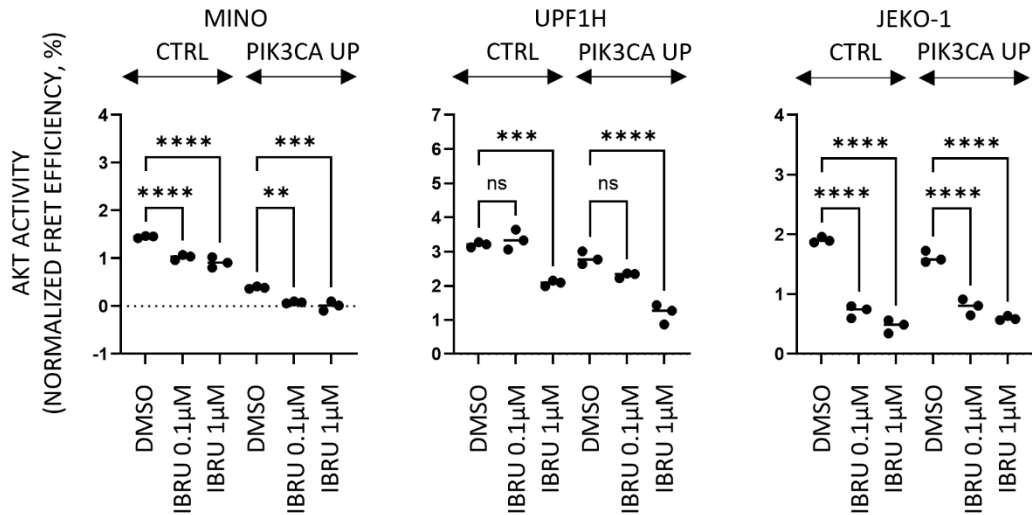
226

227 **Supplemental figure 8.** AKT activity as measured using genetically encoded FRET-based biosensor. AKT
 228 activity in *PTEN* KO cells is higher compared to respective unmodified cell lines. After exposure to BTK
 229 inhibitor ibrutinib for 3 hours (0.1 μ M, 1 μ M), AKT activity in *PTEN* KO cells remains higher than AKT
 230 activity in the respective CTRL cell lines; “ns” means “not significant”, * $p < 0.05$, ** $p < 0.01$, *** $p < 0.001$,
 231 **** $p < 0.0001$; N=3; (N) represents the number of biological replicates.



232
 233 **Supplemental figure 9.** AKT activity as measured by genetically encoded FRET-based biosensor in
 234 MINO *PTEN* KD cells after ibrutinib. AKT activity in *PTEN* KD cells is higher compared to respective
 235 unmodified cells. After exposure to BTK inhibitor ibrutinib for 3 hours (0.1 μ M, 1 μ M), AKT activity in
 236 *PTEN* KD cells remains higher with the 0.1 μ M ibrutinib than in the respective CTRL cell line with 0.1
 237 μ M ibrutinib; “ns” means “not significant”, * $p < 0.05$, ** $p < 0.01$, *** $p < 0.001$, **** $p < 0.0001$; N=3; (N)
 238 represents the number of biological replicates.

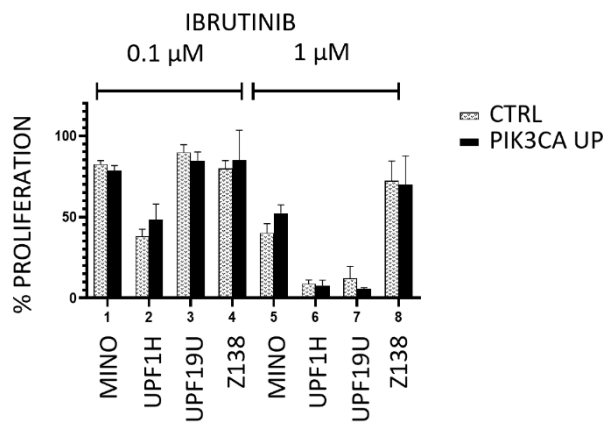
239



240

241 **Supplemental figure 10.** AKT activity is measured using genetically encoded FRET-based biosensor.
 242 Measurement of AKT activity after Ibrutinib (3 hours exposure) in 3 *PIK3CA* UP cell lines UPF1H, MINO
 243 and JEKO-1 by FRET assay showing that Ibrutinib decreases AKT activity in *PIK3CA* UP cell lines more
 244 than in CTRL in two of them; “ns” means “not significant”, ** p<0.01, *** p<0.001, **** p<0.0001.
 245 N=3; (N) represents the number of biological replicates.

246



247

248 **Supplemental figure 11.** Proliferation assay implemented 72 hours after exposure to Ibrutinib (0.1, 1
 249 µM), the cellular proliferation of the treated cells was normalized to the cellular proliferation of the
 250 untreated cells; N=3; data are represented as means ± SD.

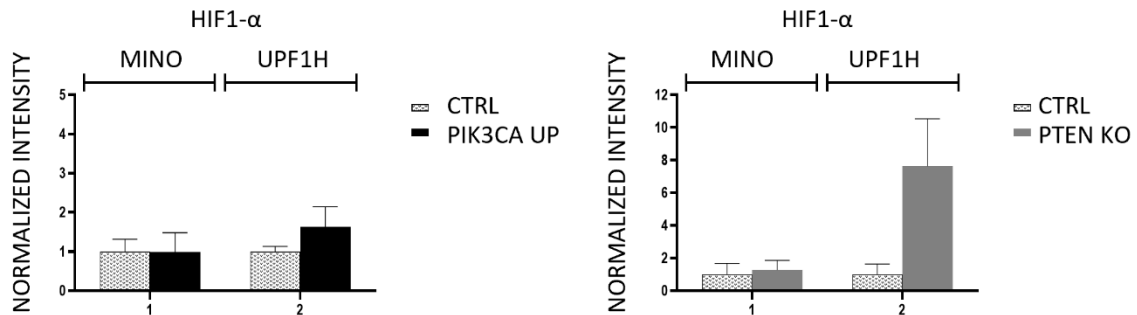
251



252

253 **Supplemental figure 12.** Number of apoptotic cells 24 hours after exposure of MINO and MINO KD cell
 254 lines to the glycolysis inhibitor 2-deoxy-D-glucose (2.5, 5, 7.5 mM). Apoptosis of the treated cells was
 255 normalized to the apoptosis of the untreated cells. N=3. Data are represented by means \pm SD. (N)
 256 represents the number of biological replicates.

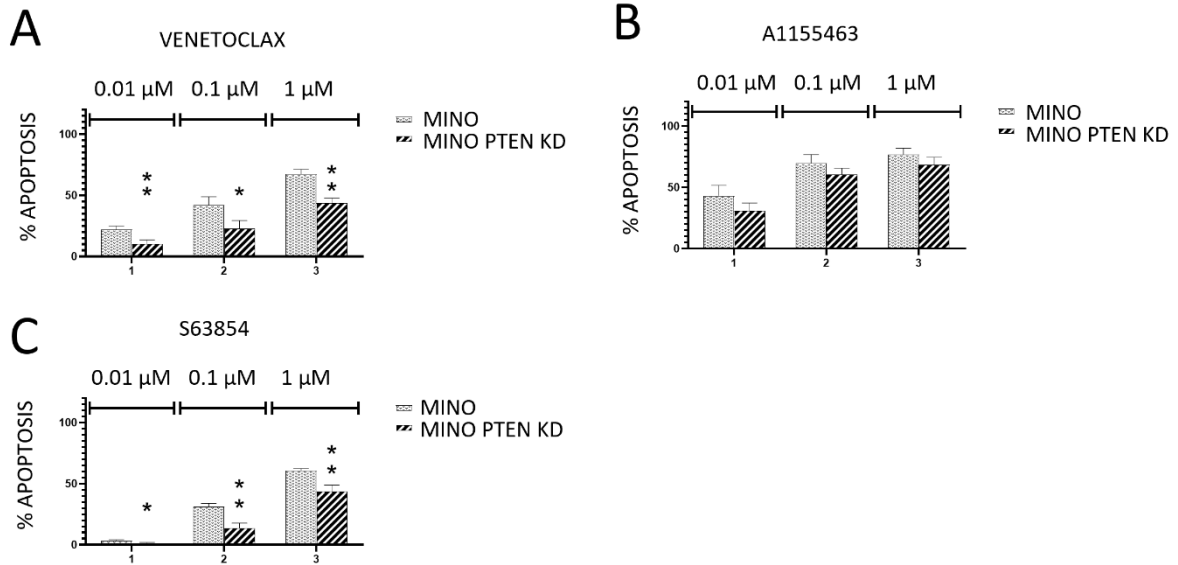
257



258

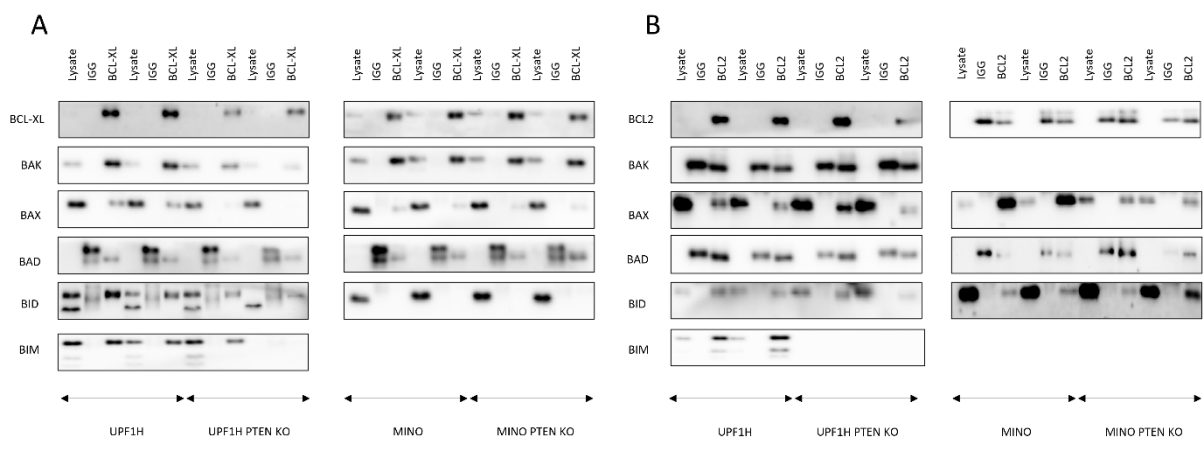
259 **Supplemental figure 13.** Quantification of HIF1- α expression in MINO PIK3CA UP, MINO PTEN KO,
 260 UPF1H PIK3CA UP, UPF1H PTEN KO and their respective controls. The values are normalized to each
 261 cell line's respective control.

262



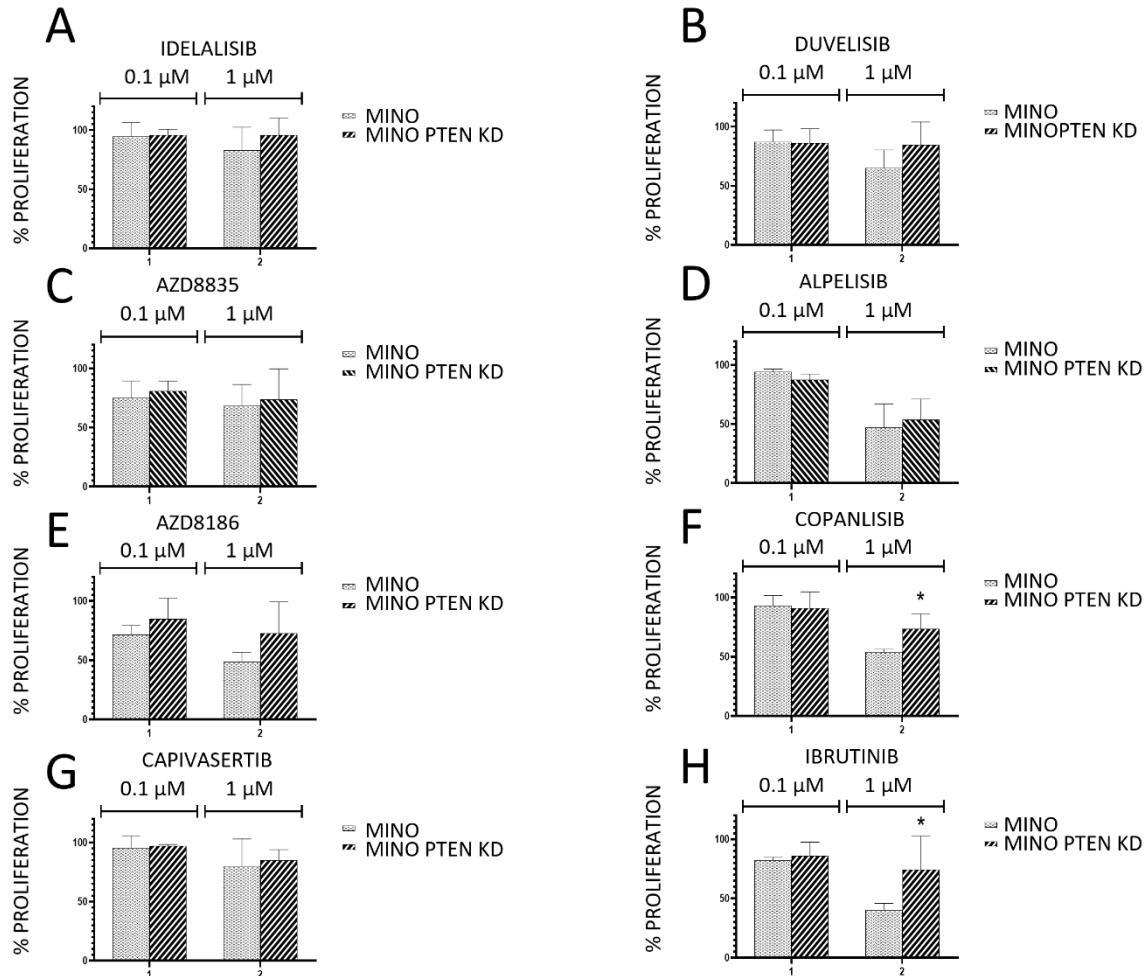
263
264
265
266
267
268
269
270

Supplemental figure 14. Number of apoptotic cells 24 hours after exposure of MINO and MINO KD cell lines to the BH3 mimetics venetoclax (0.01, 0.1, 1 μM), S63845 (0.01, 0.1, 1 μM), and A1155463 (0.01, 0.1, 1 μM). Apoptosis of the treated cells was normalized to the apoptosis of the untreated cells. N=3. data are represented by means ± SD; * p<0.05, ** p<0.01; (N) represents the number of biological replicates.



271
272
273
274
275
276
277
278

Supplemental figure 15. Co-immunoprecipitation of BCL-XL and BCL2. (A) Decreased interaction of BIM with BCL-XL in UPF1H and MINO *PTEN* KO. (B) Decreased interaction of BAX with BCL2 in UPF1H and MINO *PTEN* KO. Decreased interaction of BIM with BCL2 in UPF1H *PTEN* KO; for each sample N=2; (N) represents the number of biological replicates. The interaction of BAK with BCL2 was not measured for MINO versus MINO *PTEN* KO since BAK doesn't bind BCL2 in MINO cell line as previously shown (10) MINO has biallelic deletion of BIM.



279

280

281 **Supplemental figure 16.** Proliferation assays implemented 72 hours after exposure of MINO and MINO
 282 KD to the indicated agents: (A) Idelalisib (1, 10 μM), (B) Duvelisib (1, 10 μM), (C) AZD8835, (D) AZD8186
 283 (1, 10 μM), (1, 10 μM), Alpelisib (1, 10 μM), Copanlisib (0.01, 0.1 μM), Capiasertib (1, 10 μM); the
 284 cellular proliferation of the treated cells was normalized to the cellular proliferation of the untreated
 285 cells; N=3; data are represented as means ± SD; * p<0.05, ** p<0.01, *** p<0.001, **** p<0.0001; (N)
 286 represents the number of biological replicates.

287

288 SUPPLEMENTAL REFERENCES

- 289 1. Havranek O, Xu J, Kohrer S, Wang Z, Becker L, Comer JM, et al. Tonic B-cell receptor signaling in
 290 diffuse large B-cell lymphoma. *Blood*. 2017;130(8):995-1006.
- 291 2. Ran FA, Hsu PD, Lin CY, Gootenberg JS, Konermann S, Trevino AE, et al. Double nicking by RNA-
 292 guided CRISPR Cas9 for enhanced genome editing specificity. *Cell*. 2013;154(6):1380-9.
- 293 3. Cong L, Ran FA, Cox D, Lin S, Barretto R, Habib N, et al. Multiplex genome engineering using
 294 CRISPR/Cas systems. *Science (New York, NY)*. 2013;339(6121):819-23.
- 295 4. Henderson J, Havranek O, Ma MCJ, Herman V, Kupcova K, Chrbolkova T, et al. Detecting Förster
 296 resonance energy transfer in living cells by conventional and spectral flow cytometry. *Cytometry Part*
 297 *A : the journal of the International Society for Analytical Cytology*. 2021.

- 298 5. Kowarz E, Loscher D, Marschalek R. Optimized Sleeping Beauty transposons rapidly generate
299 stable transgenic cell lines. *Biotechnology journal*. 2015;10(4):647-53.
- 300 6. Prukova D, Andera L, Nahacka Z, Karolova J, Svaton M, Klanova M, et al. Cotargeting of BCL2
301 with Venetoclax and MCL1 with S63845 Is Synthetically Lethal. *Clin Cancer Res*. 2019;25(14):4455-65.
- 302 7. Mates L, Chuah MK, Belay E, Jerchow B, Manoj N, Acosta-Sanchez A, et al. Molecular evolution
303 of a novel hyperactive Sleeping Beauty transposase enables robust stable gene transfer in vertebrates.
304 *Nature genetics*. 2009;41(6):753-61.
- 305 8. Klanova M, Lorkova L, Vit O, Maswabi B, Molinsky J, Pospisilova J, et al. Downregulation of
306 deoxycytidine kinase in cytarabine-resistant mantle cell lymphoma cells confers cross-resistance to
307 nucleoside analogs gemcitabine, fludarabine and cladribine, but not to other classes of anti-lymphoma
308 agents. *Mol Cancer*. 2014;13:159.
- 309 9. Klanova M, Andera L, Brazina J, Svadlenka J, Benesova S, Soukup J, et al. Targeting of BCL2
310 Family Proteins with ABT-199 and Homoharringtonine Reveals BCL2- and MCL1-Dependent Subgroups
311 of Diffuse Large B-Cell Lymphoma. *Clin Cancer Res*. 2016;22(5):1138-49.
- 312 10. Dolnikova A, Kazantsev D, Klanova M, Pokorna E, Sovilj D, Kelemen CD, et al. Blockage of BCL-
313 XL overcomes venetoclax resistance across BCL2+ lymphoid malignancies irrespective of BIM status.
314 *Blood Adv*. 2024;8(13):3532-43.

315